J|A|C|S
COMMUNICATIONS

Published on Web 06/05/2004

Detection-Dependent Kinetics as a Probe of Folding Landscape Microstructure

Wei Yuan Yang and Martin Gruebele*

Center for Biophysics and Computational Biology and Departments of Chemistry and Physics, University of Illinois at Urbana-Champaign, Illinois 61801

Received February 4, 2004; E-mail: weiyang@fas.harvard.edu; gruebele@scs.uiuc.edu

The folding landscapes of polypeptides and proteins exhibit a hierarchy of local minima.[1] The causes range from proline isomerization (large free energy barrier),[2] to kinetic intermediates,[3,4] down to microstructure in the free energy caused by residual frustration inherent even in the best 20 amino acid design (<3 kT barriers).[5,6] The corresponding time scales range from hours to submicroseconds. The smallest microstructures are difficult to detect: ensemble experiments detect only the main barrier crossing(s), while single-molecule techniques currently cannot reach the required submicrosecond time scale. We measured the folding/unfolding kinetics of trpzip2 peptide at different tryptophan fluorescence wavelengths. Each measurement yielded a different rate. Wavelength-dependent folding kinetics on 0.1−2 μs time scales show that different microstructures with a range of solvent exposure and local dynamics are populated. We estimate a lower limit for the roughness of the free energy from the range of rates observed.

Very fast folding peptides and proteins provide the best candidates for finding signatures of energy landscape microstructure in folding kinetics because their main barrier is very small.[7] A fast phase preceding the activated folding kinetics of the 80-residue protein λ_{6-85} has been assigned to diffusive hopping limited by free energy microstructure,[8] but the different spectroscopic signatures one might expect from different microstructures have not yet been differentiated during folding/unfolding kinetics.

With Swope and Pitera, we recently characterized the folding thermodynamics of the β-hairpin peptide trpzip2 constructed by Cochran et al. by experiment and replica exchange molecular dynamics [9,10] The trpzip2 free energy landscape is rugged with local minima (other than the native state) ranging from 1 to 4 kT at 310 K (Figure 1). Although individual thermal titrations appear cooperative, different spectroscopic probes yielded a range of apparent unfolding temperatures, which were assigned to processes ranging from loosening of the tryptophan side chains (<30 °C) to breakup of the mini-core largely composed of tryptophans (>50 °C).

In addition to having a favorable landscape for observing free energy microstructure, trpzip2 contains four tryptophans whose fluorescence wavelength is solvation-dependent. Different local minima of trpzip2 differ in solvent exposure and are probed to differing extents by the tryptophans (Figure 1).[10] As they are populated during folding, the microstructures could manifest themselves via wavelength-dependent kinetics. Each time scale revealed by dynamics represents one or more microstructures observed. Whether local minima are populated sequentially (homogeneously) or in parallel (heterogeneously in different molecules, Figure 1), the different time scales contain information on local barrier heights and diffusion times.

Trpzip2 was prepared as previously described.[8] We induced population relaxation among its free energy minima with a nanosecond laser temperature jump of 11−13 °C.[11] Different fluorescent wavelengths were monitored by using different combinations of filters (Hoya U340, UV32, UV30, and B390). Low UV excitation energy and concentrations below 11 μM were used to avoid tryptophan photobleaching and intermolecular effects (see Supporting Information for details). No reconfiguration of the experiment was required for different probe wavelengths so that small changes in folding times could be determined reliably.

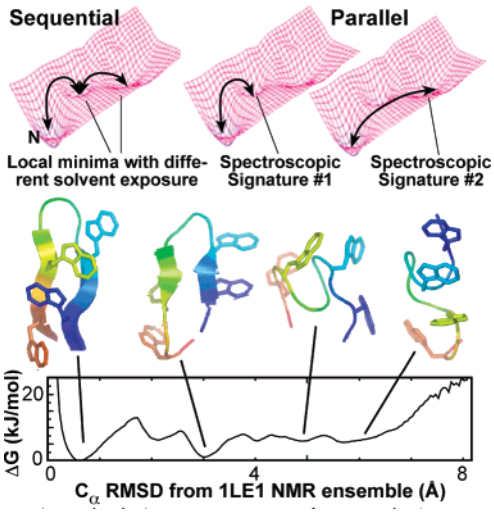

Figure 1. (Top) Local microstructures on a 2-D free energy landscape, populated homogeneously or heterogeneously, can be differentiated if their spectroscopic signatures differ, and if no large barrier hides them. (Bottom) 1-D free energy landscape and representative structures of trpzip2 from ref 10, with the root-mean-square deviation of the C_α carbons as reaction coordinate.

Relaxation of trpzip2 displays at least two groups of time scales in 0−2 M GuHCl, independently of the protein concentration (Figure 2). Within the first 100 ns, the fastest process leads to a rapid increase of trpzip2 fluorescence. Within 0.6−5 μs (depending on temperature and denaturant), the slower process completes the kinetics, leading to the equilibrium fluorescence signature. Several additional kinetic transients at different temperatures and denaturant concentrations are shown in the Supporting Information.

Our key result is that the rate of the microsecond process depends on which spectral region of the trpzip2 fluorescence emission is collected. This is illustrated in Figure 2. The relaxation time is faster at the red end of the spectrum, corresponding to more solvent-exposed tryptophan residues. Another interesting result is summarized in Figure 3: the wavelength-dependent discrepancy in the kinetics increases as the temperature is raised from 30 to 60 °C. The ca. 0.7 μs folding time in 0 M GuHCl at 25 °C (see Supporting Information) makes trpzip2 a very fast folder, but without a well-defined rate constant.

The spectroscopic and kinetic signatures of the nanosecond and microsecond processes match up in several ways with the two broad

10.1021/ja0493751 CCC: $27.50

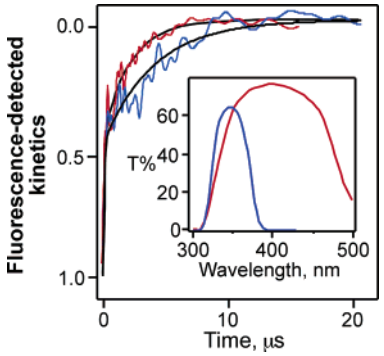

Figure 2. Relaxation dynamics of trpzip2 in aqueous 2 M guanidinium buffer monitored at 57.5 ± 1 °C in two different wavelength regions (blue: Hoya U340 + UV32 filters, $k_{slow} = 0.37\ \mu s^{-1}$; red: Hoya B390 + UV30 filters, $k_{slow} = 0.47\ \mu s^{-1}$) under otherwise identical conditions. The ns phase acounts for half of the signal.

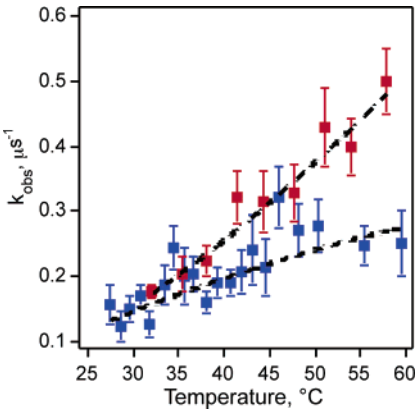

Figure 3. Temperature dependence of the μs process corresponding to the two wavelength ranges in Figure 2. The dotted curves are fits to a quadratic expansion of the apparent activation energy (Supporting Information).

transition regions observed during thermal denaturation,[10] and so we assign the two dynamical processes accordingly.

We attribute the nanosecond process to a loss of tryptophan side-chain ordering: Its amplitude decreases between 30 and 60 °C (Supporting Information), matching the thermal transition of trpzip2 side-chain flexibility reported by fluorescence intensity measurements and molecular dynamics simulation.[10] The faster phase always corresponds to a fluorescence increase, as expected from increased tryptophan mobility (Figure 2).[12] Finally, its rate is insensitive to GuHCl concentration, and so is the thermodynamic transition to increased tryptophan flexibility as monitored by fluorescence.[10]

The wavelength-dependent μs phase of main interest here comes from breaking up the tryptophan−tryptophan mini-core: Its rate and amplitude are sensitive to GuHCl concentration, in analogy to the core melting probed by steady-state CD measurements.[10] Its amplitude relative to the fast phase grows as the temperature is increased above 50 °C, matching the trpzip2 core melting transition at 50−70 °C.

A final observation ties in nicely with this assignment. Trpzip2 molecules with red-shifted fluorescence are more unfolded,[10] yet they relax to equilibrium up to 2.2 times faster than the trpzip2 molecules with blue-shifted fluorescence (Figure 3). Nearly folded conformations are more likely to be trapped in local minima (e.g. incorrect tryptophan pairings or incorrectly oriented aromatic stacks). Thus, more unfolded molecules can end up folding faster than more compact but trapped structures. The dynamics in Figure 3 speed up as the temperature is raised because more of the extended structures are populated at higher temperature, whereas at low temperatures most of the molecules reside in more compact trapped states.[10]

A very simple model serves to illustrate the type of information that can be extracted with more sophisticated theory. Let us assume that escape rates from individual local minima can be modeled by a transition state theory, $k_i = \nu_i^{\dagger}\exp(-\Delta G_i^{\dagger}/kT)$ (strictly valid only for barriers ≫1 kT), and that the prefactors are similar for all microstructures (in reality local diffusion coefficients depend on the reaction coordinate), so all roughness is contained in the activation term.[13] Then

$$\overline{(kT)^2 \ln(k_i/k_j)^2} = \overline{(\Delta G_i^{\dagger} - \Delta G_j^{\dagger})^2} = \delta^2 G \qquad (1)$$

characterizes the fluctuations in free energy. Using our value $k_i/k_j = 2.2$ near the melting midpoint as an estimate for the true average yields $\delta^2 G \approx 0.6k^2T^2$. This provides a lower limit (broadband fluorescence detection averages over ensembles, reducing the spread of rates), but the important point for more accurate modeling is that free energy roughness must be characterized by the size of its root-mean-square fluctuations,[5] not by an average value. An average value is meaningful only for a single, well-defined barrier.

Trpzip2 is thus an ideal candidate for analytical models, off-lattice simulations, and molecular dynamics calculations to probe folding free energy microstructure in more depth. To provide additional data, it will be worthwhile to add more spectroscopic probes, such as IR-detected temperature jumps, which could resolve dynamics in more detail with the help of isotope substitution, as shown in ref 14. [Note added in proof, see ref 15.]

Acknowledgment. This work was funded by NSF Grant MCB 0316925.

Supporting Information Available: Experimental details. This material is available free of charge via the Internet at http://pubs.acs.org.

References

(1) Frauenfelder, H.; Sligar, S. G.; Wolynes, P. G. *Science* **1991**, *254*, 1598−1603.
(2) Kelley, R. F.; Richards, F. M. *Biochemistry* **1987**, *26*, 6765−6774.
(3) Kim, P. S.; Baldwin, R. L. *Annu. Rev. Biochem.* **1990**, *59*, 631−660.
(4) Tezcan, F. A.; Findley, W. M.; Crane, B. R.; Ross, S. A.; Lyubovitsky, J. G.; Gray, H. B.; Winkler, J. R. *Proc. Natl. Acad. Sci. U.S.A.* **2002**, *99*, 8626−8630.
(5) Bryngelson, J. D.; Wolynes, P. G, *J. Phys. Chem.* **1989**, *93*, 6902−6915.
(6) Shea, J. E.; Onuchic, J. N.; C L Brooks, I. *J. Chem. Phys.* **2000**, *113*, 7663−7671.
(7) Eaton, W. A.; Muñoz, V.; Thompson, P. A.; Henry, E. R.; Hofrichter, J. *Acc. Chem. Res.* **1998**, *31*, 745−753.
(8) Yang, W. Y.; Gruebele, M. *Nature* **2003**, *423*, 193−197.
(9) Cochran, A. G.; Skelton, N. J.; Starovasnik, M. A. *Proc. Natl. Acad. Sci. U.S.A.* **2001**, *98*, 5578−5583.
(10) Yang, W. Y.; Pitera, J.; Swope, W.; Gruebele, M. *J. Mol. Biol.* **2004**, *336*, 241−251.
(11) Ballew, R. M.; Sabelko, J.; Reiner, C.; Gruebele, M. *Rev. Sci. Instrum.* **1996**, *67*, 3694−3699.
(12) Ervin, J.; Larios, E.; Osvath, S.; Schulten, K.; Gruebele, M. *Biophys. J.* **2002**, *83*, 473−483.
(13) Klimov, D. K.; Thirumalai, D. *Proc. Natl. Acad. Sci. U.S.A.* **2000**, *97*, 2544−2549.
(14) Huang, C. Y.; Getahun, Z.; Wang, T.; DeGrado, W. F.; Gai, F. *J. Am. Chem. Soc.* **2001**, *123*, 12111−12112.
(15) Snow, C. D.; Qiu, L. L.; Du, D. G.; Gai, F.; Hagen, S. J.; Pande, J. S. *Proc. Natl. Acad. Sci. U.S.A.* **2004**, *101*, 4077−4082.

JA0493751